# Polymeric Nanocomposites for Tribological Applications

David L. Burris, Benjamin Boesl, Gerald R. Bourne, W. Gregory Sawyer*

Polymer nanocomposites operate in applications where fluid and grease lubricants fail, and have superior tribological performance to traditional polymer composites. Nanoparticle fillers have been a part of notable reductions in the wear rate of the polymer matrix at very low loadings. Despite instances of remarkable wear reductions at unprecedented loadings (3 000 times at 0.5% loading in one case), there is a lack of general agreement within the literature on the mechanisms of wear resistance in these nanocomposites. In addition, results appear to vary widely from study to study with only subtle changes of the filler material or blending technique. The apparent wide variation in tribological results is likely a result of processing and experimental differences. Tribology is inherently complex with no governing laws for dry sliding friction or wear, and the state of the art in polymeric nanocomposites tribology includes many qualitative descriptors of important system parameters, such as particle dispersion, bulk mechanical properties, debris morphology, and transfer film adhesion, morphology, composition, and chemistry. The coupling of inherent tribological complexities with the complicated mechanics of poorly characterized nanocomposites makes interpretation of experimental results and the state of the field extremely difficult. This paper reviews the state of the art in polymeric nanocomposites tribology and highlights the need for more quantitative studies. Examples of such quantitative measurements are given from recent studies, which mostly involve investigation of polytetrafluoroethylene matrix nanocomposites.

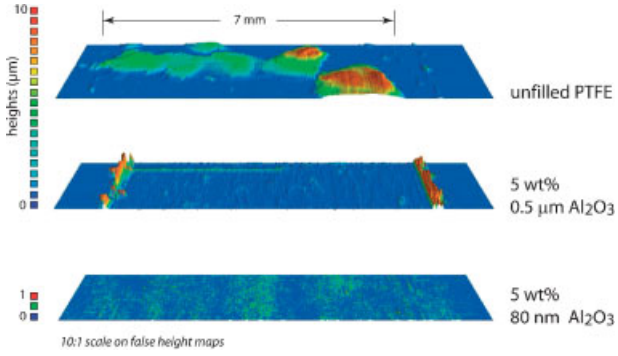


## Tribology and Polymer-Based Solid Lubrication

### Composites in Tribology

Polymer composites are well known for offering engineers high strength-to-weight ratios and flexibility in material design.[1,2] The physical properties of a composite can be tuned to satisfy various functional requirements of a target application, including stiffness and strength, thermal and electrical transport, and wear resistance to name a few. Often, composites are designed to fulfill several functions simultaneously.

One area of engineering that is particularly invested in the development and design of high performance polymer composites is tribology, the science related to interacting surfaces in relative motion. Bearings are systems that contain sliding interfaces, and are relied upon by nearly all moving mechanical systems. Though rarely recognized,

D. L. Burris, B. Boesl, G. R. Bourne, W. G. Sawyer
Department of Mechanical and Aerospace Engineering, University of Florida, Gainesville FL 32611, USA
E-mail: wgsawyer@ufl.edu



DOI: 10.1002/mame.200600416

**David Burris** has a B.Sc. and an M.Sc. degree from the University of Florida, obtained in 2003 and 2006 respectively. He is currently a doctoral candidate at the University of Florida working on solid lubrication in extreme environments. David has authored 13 journal publications, and has 7 international patents.

**Ben Boesl** is a doctoral student at the University of Florida working on solid lubrication in extreme environments. His interests are in microscopy, fracture, and characterization of sparse distributions in nanoparticle-filled polymeric composite systems.

**Jerry Bourne** has a Ph.D. from the University of Florida in Materials Science and Engineering 2006. He is currently a member of the technical staff at the Major Analytical and Instrumentation Center at the University of Florida. His research interests are in microscopy, the limits of solid lubrication theory, and the metallic glass systems.

**Gregory Sawyer** is an Associate Professor in the Department of Mechanical and Aerospace Engineering. His primary interests are in tribology, particularly solid-lubrication and sliding contacts in extreme environments, where the use of fluid lubrication is not available.

the performance of these systems is often critically dependent on the performance of its bearings, which can depend strongly on the lubricant, operating conditions, and the environment. There continues to be demand for performance in environments and applications where the use of liquid lubricants is undesirable or even precluded. Such environments can include ultra-high vacuum, high and low temperatures, corrosive chemicals, abrasives, and radiation to name a few.[3–9] Failure of the lubricant or unpredictable behavior at the interface can lead to device and system failure. Solid lubricants are increasingly applied and enable successful operation in extreme climate and environments. Solid lubrication has a number of advantages, which include simplicity, reduced cost, cleanliness, and ease of implementation.[10–13] Unfortunately, because solid lubricants often sacrifice material to provide low friction they wear during operation and life is limited because of the rates of wear. Composites are often created to increase the wear resistance of a particular polymer matrix. In recent years, there have been a number of successful composites made by blending nanofillers in polymeric matrices.[14–35]

## Tribometry

Friction coefficients and wear rates are often discussed in tribology. Friction coefficients can dictate required motor torques and loads. Wear can lead to debris generation, binding, slop, and limited life. Because of the important role of each in design, they are the primary metrics of performance in tribological systems and are quantified in most tribological studies.

A friction coefficient, $\mu$, is defined as a ratio of the force that resists sliding to the normal force. A tribometer is a device used to measure friction coefficients. While there is no standard tribometry test, experimental setups generally utilize similar design philosophies. In its simplest form, a flat solid lubricant sample is slid against the flat surface of a much larger and harder block of material called the counterface. This results in an approximately uniform pressure distribution in the solid lubricant. In many cases, the counterface material and surface finish are important factors in system performance. For transfer-film-forming solid lubricants, these factors may play a less critical role. Transfer films can form through mechanical interlocking of plastically deformed debris, adhesion, or direct chemical bonding of the polymer with the bare counterface. These films are critical to the performance of a solid lubricant. They reduce wear by shielding the softer solid lubricant from direct asperity contact and they reduce friction by providing low shear strength for motion accommodation during sliding.[36–42] Upon sliding, the frictional and normal forces are measured or inferred at the specimen simultaneously. A detailed uncertainty analysis of the measurement of friction coefficient on a similar pin-on-flat tribometer was performed by Schmitz et al.,[43] and illustrates the metrology challenges associated with such a seemingly simple measurement.

Wear rate, $k$, is defined as the volume of material removed per unit of normal load per unit distance of sliding, with typical units being $mm^3 \cdot N^{-1} \cdot m^{-1}$. Values of wear rates for solid lubricants used in application can vary by several orders of magnitude. Since volumetric measurements can not practically cover this range, the test length often becomes a function of the wear rate being measured (loads are usually held constant). For example, in experiments that vary polyetheretherketone (PEEK) content in a polytetrafluoroethylene (PTFE) matrix, the unfilled PTFE was completely consumed in 2 h with 200 mg of mass loss, while a composite sample required nearly a week of continuous testing to lose the 10 μg resolution of the scale.[44] Reporting the experimental uncertainty is necessary to indicate the quality of measurement, and is especially important when wear rates are low. Calculations of normal load and sliding distance with associated uncertainties are fairly straightforward, but measurements of volume loss often require more careful consideration. For materials that do not uptake or outgas, material mass measurements are typically made because dimensional distortions caused by elasticity, plasticity, creep, and thermal fluctuations can confound dimensional measurements of wear. Density can be calculated by making an initial sample mass measurement with dimensional measurements or with another direct measurement of volume. Schmitz et al.[45] performed a detailed uncertainty analysis of wear rate measurement for a pin-on-flat tribometer.


*Macromol. Mater. Eng.* **2007**, *292*, 387–402

Macromolecular Journals

DOI: 10.1002/mame.200600416

### Solid Lubricants

Figure 1 is a graph that shows wear rate plotted versus friction coefficient for various unfilled polymers, polymer blends, and polymer composites used in tribology studies.[14–16,20,27,30,32,44,46–49] While tribological performance does not have a single unique definition, broadly speaking, materials with low wear rates and low friction coefficients are desirable. For practical purposes a designer might include constant performance guidelines (Figure 1 illustrates how such guidelines might be used) whose slopes depend on the relative importance of friction coefficient and wear rate for a specific application (note wear rates are on a log scale). High performance engineering polymers like PEEK and polyimide (PI) have good wear resistance but high friction coefficients, while low friction materials like PTFE usually have prohibitively high wear rates. In general, neat polymers lack the tribological performance required for most applications; there are many examples of polymer composites in tribology.

One philosophy of material design in tribology is to improve the frictional behavior of a wear resistant polymer. For example, additions of PTFE to PEEK have been found to significantly reduce friction coefficients; this often results in reduced wear.[32,50–52] The opposite method is also employed where hard particle and fiber fillers are used to reduce the wear of a low-friction high-wear material like PTFE, often at the expense of friction coefficient.[53–56] There are significant efforts dedicated to the research and development of low-friction low-wear solid lubricants with traditional particle and fiber fillers, many of which have successfully transferred to application. Friedrich et al.[52] and Zhang[57] reviewed the state of the art of polymer composites in tribology in 1995 and 1998, respectively.

## Nanocomposites in Tribology

One drawback of the hard micrometer-sized particle and fiber fillers frequently used to reinforce polymers is that they tend to abrade the counterface. This prevents the formation of a protective transfer film,[36] increases the friction coefficient and counterface roughness, and leads to third body wear of the composite. The recent availability of nanoparticles (defined as a particle with characteristic dimensions of less than 100 nm) has initiated much enthusiasm within the community because they have the potential to reduce the abrasion that leads to these cascading and problematic events. Because nanoparticles are of the same size scale as counterface asperities, they may polish the highest asperities and promote the development of tribologically favorable transfer films. Once formed, the transfer films shield the composite from direct asperity contact and damage.[36]

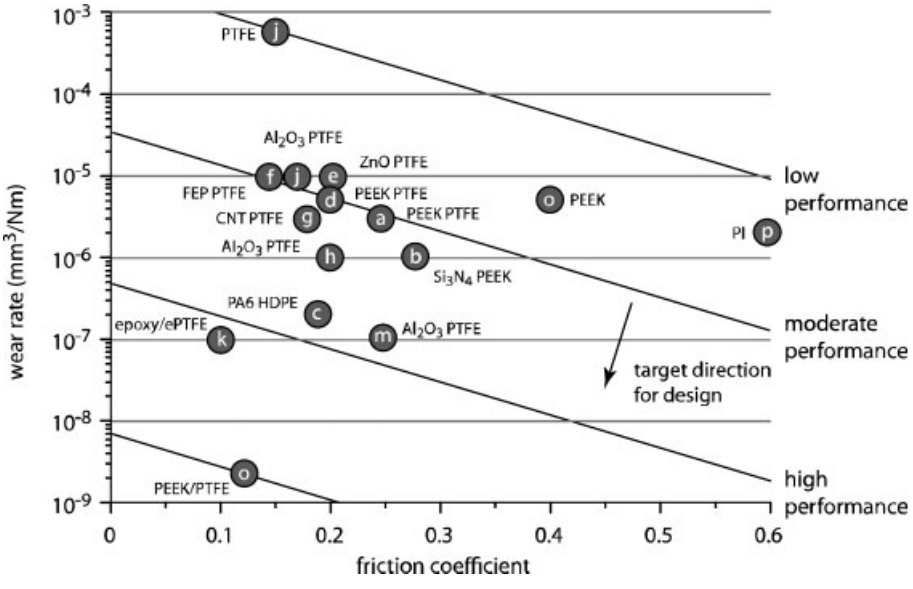


*Figure 1.* A multivariate plot of wear rate (*y* axis) versus friction coefficient (*x* axis) for various solid lubricating polymeric composites, unfilled polymers, and polymer blends. The target region is the lower left-hand corner, a region of ultra low wear rate and friction coefficient. The data points are labeled with the constituents and listed as (a–r): a) PTFE-PEEK composite,[46] b) $Si_3N_4$-PEEK nanocomposite,[30] c) PA6-HDPE blend,[49] d) PTFE-PEEK composite,[32] e) ZnO-PTFE nanocomposite,[20] f) FEP-PTFE composite,[48] g) CNT-PTFE nanocomposite,[16] h) $Al_2O_3$-PTFE nanocomposite,[27] j) $Al_2O_3$-PTFE nanocomposite and unfilled PTFE,[15] k) epoxy-ePTFE composite,[47] m) $Al_2O_3$-PTFE nanocomposite,[14] o) PEEK-PTFE composite and unfilled PEEK,[44] and p) unfilled PI (unpublished result), $V = 50.8$ mm·s$^{-1}$, $P = 6.25$ MPa, reciprocating pin-on-disk tribometer.

Another benefit of nanoparticles is that at low loadings (<5%), nanocomposites can have tremendous particle number densities and interfacial surface areas, and as a consequence, nanoparticles have great potential for altering matrix mechanical properties at low filler loadings. Siegel et al.[28] found that with about 2% (volume) alumina nanoparticles, the tensile strain to failure improved by 400%, and Ng et al.[23] found the scratch resistance of a $TiO_2$–epoxy nanocomposite to be superior to both unfilled and micro-filled epoxy. During strain-dependent Raman spectroscopy measurements of a multi-walled carbon-nanotube (MWCNT)-filled Lexan polycarbonate, Eitan et al.[18] found that load was transferred to the nanotubes. They also found

that an epoxide surface treatment of the nanotubes improved the load transfer through the interface, highlighting the role of the interface on mechanical properties. Nanofillers can not only improve material properties through mechanical transfer, but they can also influence the behavior of the polymer itself. Many authors have observed the direct effects of the nanoparticles on the matrix through changes in the glass transition and degradation temperatures of the polymer matrices.[25,35,58,59] Clearly, nanoparticles can influence the crystallinity, morphology, and behavior of the polymer itself and the potential for multifunctionality in these nanostructured materials is substantial. Frankly, such detailed studies of matrix properties are needed but generally lacking in the tribology literature.

Within the past decade there have been a number of studies conducted to investigate the role of nanoparticles in tribological polymer nanocomposites.[14–16,20,27,29–32,60,61] Early studies by Wang et al.[30] used nanoparticles in a PEEK matrix. The nanoparticles were dispersed in the PEEK powder by ultrasonication in an alcohol bath. In an initial study, <50 nm $Si_3N_4$ was found to be effective in reducing the wear rate and friction coefficient of PEEK. The improvements in tribological performance were mostly attributed to the vast improvements observed in the quality of the transfer films. A follow-up study looked directly at the effects of particle size and morphology on the tribological behavior of the composite.[33] Micrometer-scale whiskers, microparticles and nanoparticles of SiC were used with 5% loading in PEEK. The whiskers were effective in reducing the wear of PEEK (≈33%) but friction was only reduced ≈8%. The microparticles were effective in reducing the friction coefficient (≈33%) but the wear rate was only reduced by ≈9%. The nanoparticles effectively reduced both with a reduction in wear rate of ≈44% and a reduction in friction coefficient of ≈50%. In a later size study that involved nanometer $ZrO_2$ from 10 to 100 nm in a PEEK matrix, it was found that for approximately 2% loading, both friction coefficient and wear rate increased monotonically with filler size (improved performance of PEEK with various loadings of $SiO_2$ nanoparticles was also found).[29,31] In each of these studies, thin uniform transfer films accompanied reduced wear rates and friction coefficients.

In 2000, Schwartz and Bahadur published a study that examined the influence of alumina nanoparticles on the tribological behavior of polyphenylene sulfide (PPS).[61] Powders were dispersed with what is described as an electric mixer. A 2 times reduction of wear was observed for a 2% filled nanocomposite. They found good correlation between the bond strength of the transfer film and the wear rate of the composite and concluded that the role of the filler was to anchor the transfer film. They attributed the increased wear rates at loadings above 2% to abrasion of the transfer film by nanoparticle aggregates.

In 2001, Li et al. published a study on the tribology of PTFE filled with 50 nm ZnO.[20] Their dispersion technique was the ultrasonication of powders and particles in an acetone bath. While the friction coefficient was insensitive to ZnO nanoparticle loading, wear rate was extremely sensitive to nanoparticle loading with the addition of 15% filler reducing the wear rate of PTFE by nearly 100 times. Based on a study by Tanaka and Kawakami[62] that showed inferior wear performance of sub-micrometer $TiO_2$-PTFE composites to PTFE composites with larger sized fillers of other materials, there was a general sentiment in the field that nanofillers could not provide improvements in the wear resistance of PTFE because they would readily be swept away within the matrix as debris by relatively large asperities. The studies by Li et al. not only established that nanofillers could be as effective as microparticles in reducing the wear of PTFE at substantially lower loadings, but it also demonstrated that low friction coefficients could be retained upon loading. Uniform, well-adhered transfer films were observed for low-wear composites and no signs of abrasion to the counterface were observed.

Following this study, Chen et al. published a tribology study of a single-walled carbon nanotube (SWCNT)-PTFE nanocomposite.[16] The nanotubes were dispersed using mechanical and ultrasonic mixing in an acetone bath. This study reinforced the effectiveness of nanofillers in PTFE showing a 300 times reduction in wear at 20% loading ($3 \times 10^{-6}$ $mm^3 \cdot N^{-1} \cdot m^{-1}$). The friction coefficient monotonically decreased with increased loading up to 30% where a 15% reduction was observed. The reduction in both friction and wear were attributed to improved mechanical properties of the PTFE and the separation of the contacting surfaces by liberated nanotubes. Order of magnitude reductions in the wear rates of PTFE using fillers are relatively common.[48,51–55,63,64] As an example of this, we made a composite of PTFE and chopped beard hair; the dry sliding wear rates (6.3 MPa and 50 $mm \cdot s^{-1}$) of the 5 and 20 wt.-% beard hair samples were $2 \times 10^{-5}$ $mm^3 \cdot N^{-1} \cdot m^{-1}$ and $1 \times 10^{-6}$ $mm^3 \cdot N^{-1} \cdot m^{-1}$ respectively.

In 2003, Sawyer et al.[27] published results from alumina-PTFE nanocomposites. The study varied loading of 38 nm alumina from 0.02–10%. With as little as 0.02% loading, a 2 times increase in wear resistance was detected. Wear rate monotonically decreased with increased loading, and at 10% loading, wear was reduced by 600 times. The unique jet-mill powder dispersion technique led to reduced size and elongation of the PTFE, where 30 μm particles with close to a 1:1 aspect ratio were reduced to 5 μm with a 3:1 aspect ratio on average. These mechanically deformed PTFE particles were also observed as being decorated by the nanometer-scale alumina. The resulting microstructure after compression molding was observed using etching and secondary electron imaging; it was shown to be heterogeneous with regions of highly filled


Macromol. Mater. Eng. 2007, 292, 387–402

Macromolecular Journals
DOI: 10.1002/mame.200600416

and nominally unfilled PTFE. As the nanoparticle loading increased, the sizes and densities of the filled regions were thought to increase.

Because many thought that the effectiveness of nano-fillers was precluded because of their interactions with inherently large surface asperities during wear,[62] Burris and Sawyer conducted a study to investigate the effects of the counterface roughness on the tribology of alumina-PTFE composites.[15] Composites of varying filler size and loading were tested against surfaces whose roughnesses varied from 80 to 580 nm *R*q (root mean squared roughness). While the transient wear rate against the fresh steel surfaces was a strong function of roughness, the trend was not dependent upon filler size. In addition, at a steady state, wear rate was found to be rather insensitive to roughness, especially for transfer film formers. The role of the filler in achieving very low wear rates appeared to be the reduction of the debris size during run-in. This enabled engagement of the debris to the counterface, which initiated the formation of a protective transfer film as Bahadur and Tabor first described in 1984.[37] Once the transfer film formed to cover the asperities, the initial surface texture no longer had an effect.

## Comparisons of the Tribological Properties of Polymer Nanocomposites

Wear rate and friction coefficient are plotted versus filler loading in Figure 2 for representative polymer nanocomposites and microcomposites in the tribology literature. These studies are summarized in Table 1 by matrix, filler, literature source, dispersion technique, and optimum loading for low wear.

The testing methods, environments, and tribological conditions vary widely for the studies shown in Figure 2, so direct comparisons of the data are difficult. The normalized wear rate is defined as the ratio of the wear rate of the composite to that of the neat matrix. The normalized wear rate indicates relative improvement by

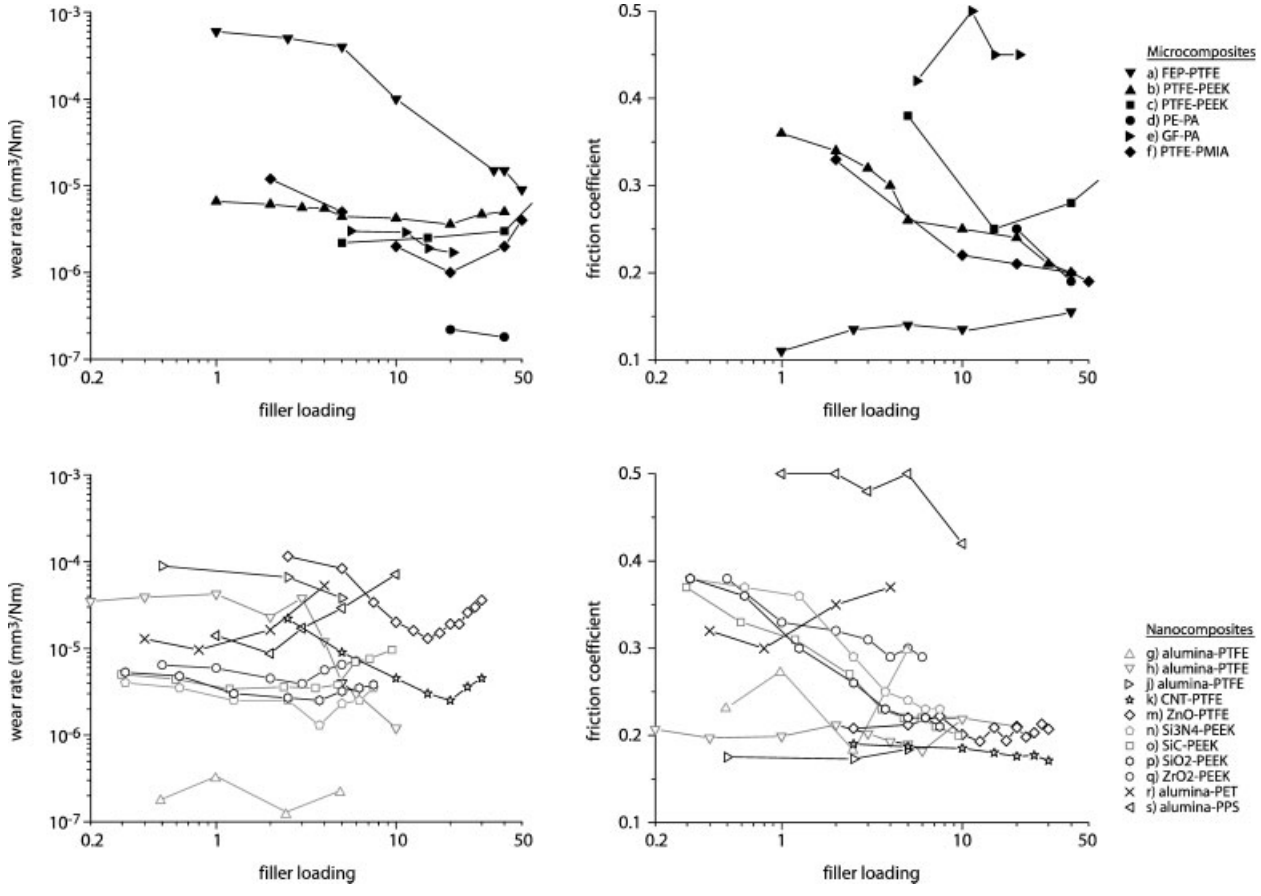


*Figure 2.* Tribological behavior of representative polymer micro- and nanocomposites in the literature. Left: wear rate plotted versus filler loading. Right: friction coefficient plotted versus filler loading. Top: microcomposites, bottom: nanocomposites. The data sets are listed as (a–s): a) FEP-PTFE composite,[48] b) PTFE-PEEK composite,[32] c) PTFE-PEEK composite,[46] d) PE-PA composite,[49] e) GF-PA composite,[63] f) PTFE-PMIA,[65] g) $Al_2O_3$-PTFE nanocomposite,[15] h),[27] j),[14] k) carbon nanotube-PTFE nanocomposite,[16] m) ZnO-PTFE,[20] n) $Si_3N_4$-PEEK nanocomposite,[30] o) SiC-PEEK nanocomposite,[32] p) $SiO_2$-PEEK nanocomposite,[29] q) $ZrO_2$-PEEK nanocomposite,[31] r) $Al_2O_3$-PET nanocomposite,[60] and s) $Al_2O_3$-PPS nanocomposite.[61]

*Table 1.* Listing of matrix, filler, author, dispersion technique and optimized loading for polymer composites (a-f) and nanocomposites (g-s) in the literature.

| Entry | Matrix | Filler | Ref. | Dispersion technique | Vol.-% at lowest wear rate |
|---|---|---|---|---|---|
| a | PTFE | FEP | [48] | mechanical | >50 |
| b | PEEK | PTFE | [32] | ultrasonication | 20 |
| c | PEEK | PTFE | [46] | N/A | 5 |
| d | PA | PE | [49] | twin screw extrusion | >40 |
| e | PA | GF | [63] | melt mixed | >20 |
| f | PMIA | PTFE | [65] | mechanical | 20 |
| g | PTFE | $Al_2O_3$ | [15] | jet mill | 0.5 |
| h | PTFE | $Al_2O_3$ | [27] | jet mill | >10 |
| j | PTFE | $Al_2O_3$ | [15] | jet mill | >5 |
| k | PTFE | CNT | [16] | ultrasonication/mechanical | 20 |
| m | PTFE | ZnO | [20] | ultrasonication/mechanical | 15 |
| n | PEEK | $Si_3N_4$ | [30] | ultrasonication | 4 |
| o | PEEK | SiC | [29] | ultrasonication | 1 |
| p | PEEK | $SiO_2$ | [29] | ultrasonication | 4 |
| q | PEEK | $ZrO_2$ | [31] | ultrasonication | 3 |
| r | PET | $Al_2O_3$ | [60] | melt mixing | 0.7 |
| s | PPS | $Al_2O_3$ | [61] | mechanical | 2 |

the filler, and is plotted versus the filler loading in Figure 3. It is desirable to maximize reductions in wear rate with minimum additions of filler. The microcomposites require 10% loading for a $\times 10$ reduction in wear rate. Loadings of microparticles around 1% have virtually no effect on the wear rate. The nanocomposites have a wide spectrum of properties. PEEK, PPS, and poly(ethylene terephthalate) (PET) matrix materials all have similar behavior with greater than 10 times reductions occurring at the optimal compositions all of which occur between 0.7 and 4% loading. At loadings above the optimum, several had diminished wear rates compared to the unfilled matrix. The PTFE matrix composites had substantially greater improvements ranging from 100- to 4 000 times. This is not entirely surprising since PTFE has the highest neat wear rate among the matrices shown. In one case, alumina nanoparticles reduced the wear of PTFE by 10 times with as little as 0.2% loading, and in another, 0.5% alumina nanoparticles reduced the wear of PTFE by 3 000 times. These composites exemplify the goal for tribological nanocomposites, namely, high wear reductions at low loadings.

While nanoparticles have demonstrated an exciting ability to impart high wear resistance to polymeric solid lubricants at low loadings, the field varies widely with maximum wear reductions varying by three orders of magnitude and optimal loadings varying by over two orders of magnitude. The factors governing these large variations have not yet been uncovered because of the general lack of bulk composite and transfer film characterization. Despite the critical role and difficulty in achieving good nanoparticle dispersion, characterization and discussion of dispersion are completely absent from the tribology literature. In many cases, improved wear resistance after nanoparticle inclusion is attributed to improved mechanical properties such as strength, hardness, and toughness without any quantitative measurement of these properties. In addition, it is common for improvements in tribological performance to be attributed to the improved transfer films. These films are qualitatively described as thin, thick, coherent, patchy, tenacious, well-adhered, or flaky and are thought to both protect the composite and provide low friction sliding.[29–33,38,39,41,53] The critical role of transfer films in tribology is universally noted by tribologists but quantitative measurements of these films are lacking.[42] Because transfer films consume composite material during formation they are coupled with the nature of the wear debris. A relatively consistent observation is that fine wear debris accompanies low wear rates. Wear debris morphologies are often used to infer modes and mechanisms of wear and are described as flaky, ribbon-like, fine, large, small, and plate-like.[41,66,67] Future studies involving quantitative measurements of critical components such as nanoparticle dispersion, filler/matrix


*Macromol. Mater. Eng.* **2007**, *292*, 387–402

Macromolecular Journals
DOI: 10.1002/mame.200600416

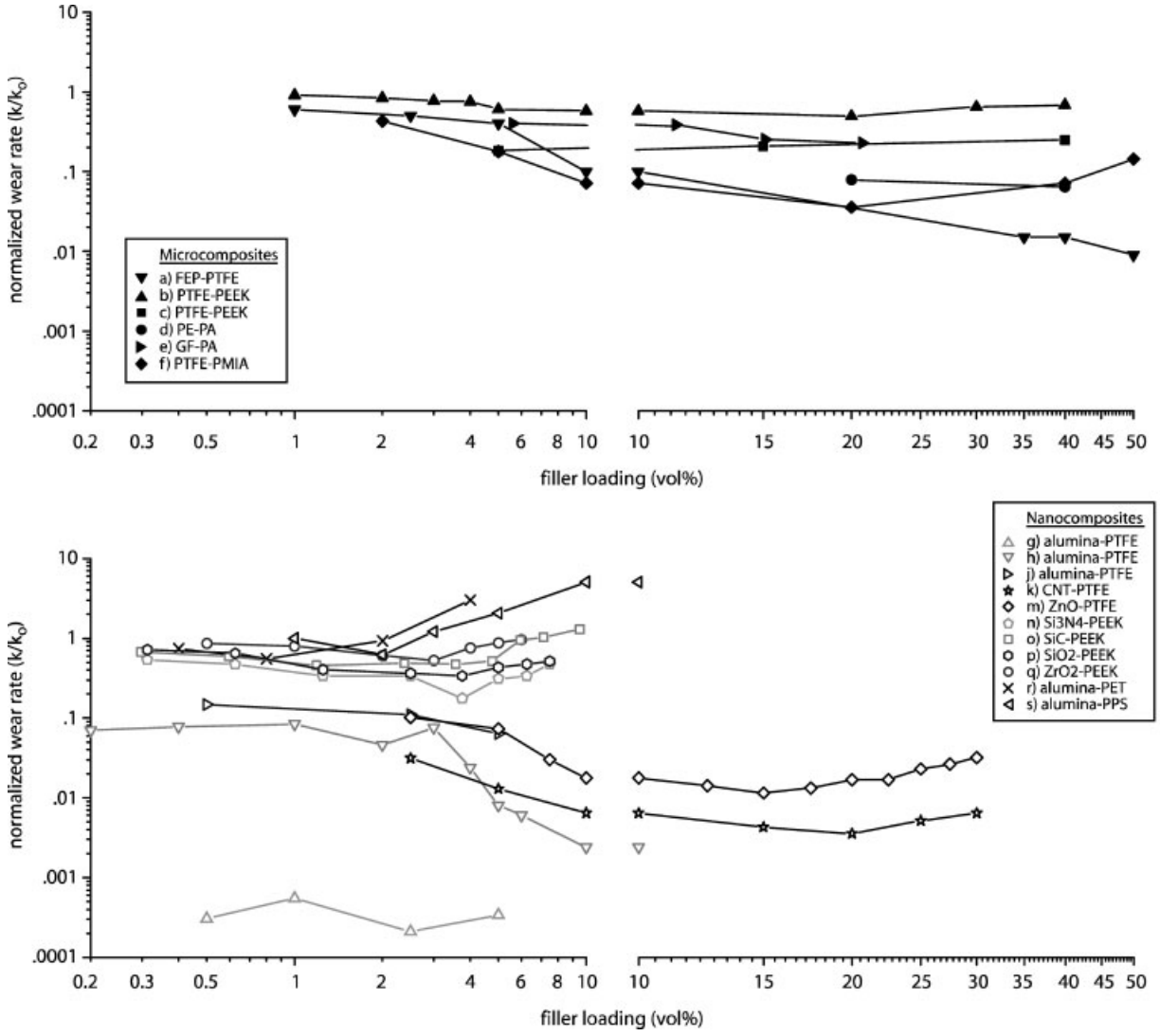


*Figure 3.* Normalized wear rate plotted versus filler loading. Normalized wear rate is defined as the ratio between the wear rate of the composite and that of the unfilled matrix. Efficient fillers impart high wear resistance at low loadings. The data sets are listed as (a–s): a) FEP-PTFE composite,[64] FEP-PTFE composite,[48] b) PTFE-PEEK composite,[32] c) PTFE-PEEK composite,[46] d) PE-PA composite,[49] e) GF-PA composite,[63] f) PTFE-PMIA,[65] g) $Al_2O_3$-PTFE nanocomposite,[15] h),[27] j),[14] k) carbon nanotube-PTFE nanocomposite,[16] m) ZnO-PTFE,[20] n) $Si_3N_4$-PEEK nanocomposite,[30] o) SiC-PEEK nanocomposite,[32] p) $SiO_2$-PEEK nanocomposite,[29] q) $ZrO_2$-PEEK nanocomposite,[31] r) $Al_2O_3$-PET nanocomposite,[60] and s) $Al_2O_3$-PPS nanocomposite.[61]

interface interactions, and transfer film properties will help elucidate causes of behavioral differences.

## The Need for Quantitative Measurement of Qualitative Observations

It is difficult to generalize the current state of nanocomposites in tribology. Many of the published nanocomposite studies focus on synthesis, characterization, or tribological evaluation; broad ranging studies that include all three of these components are missing from the literature. Often, tribologists lack the materials science background to conduct thorough nanocomposite characterization, and materials scientists lack the expertise required to conduct detailed tribological investigations of their well-characterized nanocomposites. Together, these disciplines have the complimentary tools necessary to make large impacts in this area, but to the authors' knowledge, this synergism has not yet been exploited to its full potential. Developing collaborations and sharing techniques between communities will facilitate a more comprehensive understanding of the role of nanoparticles in tribological composites. In the following sections we

will discuss some recent quantitative studies of three critical system components of primarily PTFE-based nanocomposites, namely, nanoparticle dispersion, effects of the nanoparticle–matrix interface, and transfer films.

## Characterization of Dispersion

The nanoparticle dispersion is of critical importance to the mechanical and tribological properties of the nanocomposite.[68–70] Nanoparticles have large ratios of surface forces to body forces, making their dispersion an exceedingly difficult and problematic aspect of nanocomposite synthesis. Agglomerates of nanoparticles are generally of the micrometer size-scale, so nanocomposites with agglomerations may behave as microcomposites where the filler is an ensemble of nanoparticles; thus, the potential benefits of the nanoparticles may not be realized. Characterizing the nature of the dispersion is critical in understanding the behavior of a nanocomposite. Without intimate knowledge of the agglomeration and dispersion state of a nanocomposite, interpretation of mechanical and tribological results is impossible. Despite its obvious importance in materials engineering, characterization of dispersion is virtually non-existent within the tribology literature.

In general, the nanoparticle dispersion is qualitatively assessed using descriptors such as random, good, well, uniform, homogeneous, etc... of the observed dispersion. It is difficult to capture the overall character of a particular dispersion with any single high-magnification two-dimensional image. A technique similar to tomography can be used to collect three-dimensional dispersion data by reconstructing the particle field using a series of individual slices. The challenge is to find an appropriate method to create and image the slices. One approach that we have successfully used is ion-beam milling and electron-beam imaging sequential slices through a polymer nanocomposite (each slice is approximately 30 nm thick). A reconstructed particle dispersion that was created using this technique is shown in Figure 4 for a 5 $\mu$m $\times$ 5 $\mu$m $\times$ 3 $\mu$m volume; this particular composite was an epoxy matrix filled to approximately 1 vol.-% with 53 nm ZnO nanoparticles. After reconstruction, most commercial codes can calculate a breadth of statistics, but there is no clear metric to describe dispersion.

In many systems with heterogeneous dispersion the homogeneity varies with observation size. Thus, a number of researchers use sequential scans at increasing magnification to capture the character of the dispersion. In particular, the structure and characteristic size of the agglomerations is qualitatively defined. In many cases the highest magnification suggests the best dispersion, while the lowest magnifications reveal the micrometer-scale distribution of composition for the composite. Figure 5 shows a series of such images taken using TEM from a 2 vol.-% alumina-epoxy nanocomposite. Such a technique is very useful in ascertaining the structure of the nanocomposites across a number of length scales.

There are several quantitative dispersion characterization techniques in the literature and most involve measuring interparticle spacings, number densities, and particle distributions.[17,19,68,69] The discrete nature of the particle distribution suggests that a discrete statistical treatment such as the Poisson distribution may be used to describe the spatial arrangement of nanoparticles. The Poisson distribution is used to compare random and

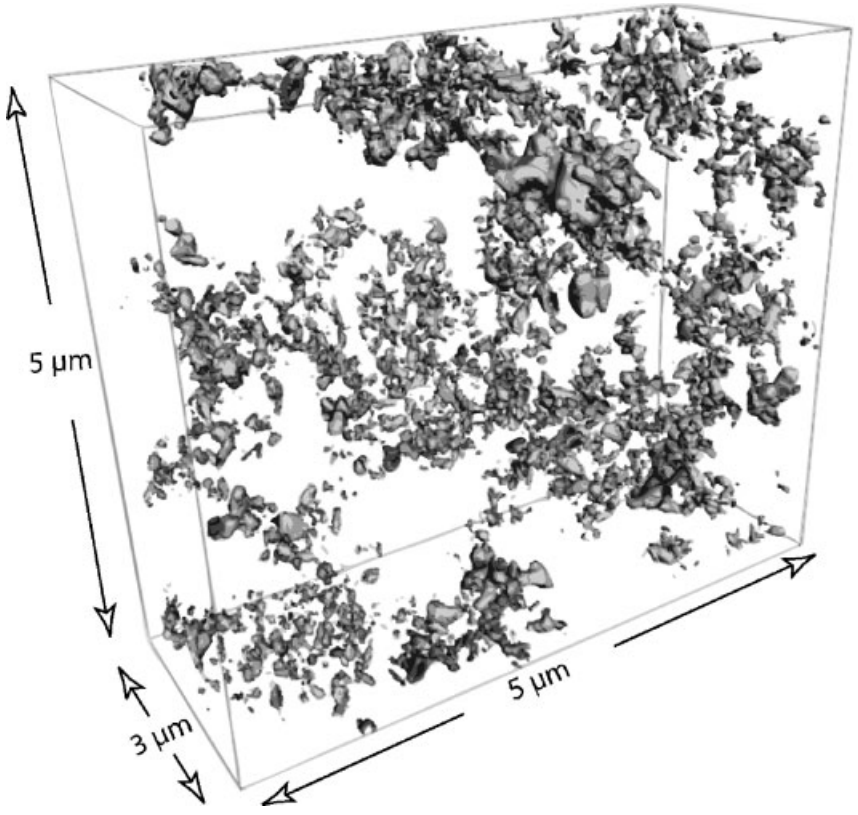


*Figure 4.* Three-dimensional reconstruction of a 1% ZnO-epoxy nanocomposite as imaged using focused-ion beam milling and a slice-and-view technique (reconstruction used 100 registered SEM images). Notice the heterogeneous nature of the particle dispersion over a volume that is 5 $\mu$m $\times$ 5 $\mu$m $\times$ 3 $\mu$m. A number of commercial codes can calculate surface area, mean free path, and particle size distributions from such data.


*Macromol. Mater. Eng.* **2007**, *292*, 387–402

Macromolecular Journals
DOI: 10.1002/mame.200600416

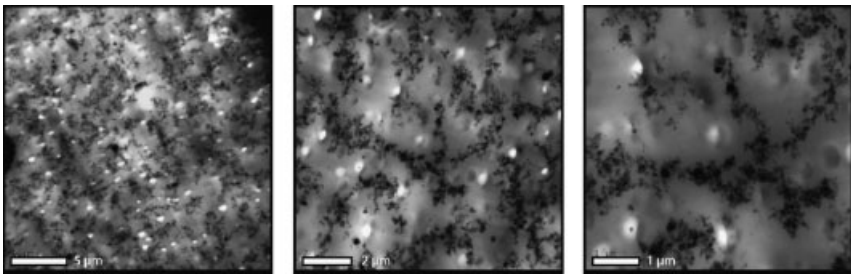


*Figure 5.* TEM images of a single domain within a 44 nm delta-gamma alumina-filled epoxy at 2 vol.-%. From left to right the images are increasing in magnification and are approximately 25, 12.5, and 6.25 μm in width. The alumina nanoparticles appear dark in the epoxy matrix.

discrete events that occur within a certain interval. In this case, the probability, $P$, of a random occurrence, $x$, as a function of area, $\lambda$, is given by Equation (1).

$$P(x;\lambda) = \frac{e^{-\lambda}\lambda^{x}}{x!} \quad (1)$$

A tedious approach that we have employed is to discretize the central locations of particles using the intensities of the digital images collected from transmission and scanning electron microscopy. Many of these images need to be manually discretized. The result of discretization is shown in Figure 6a where the lowest magnification image from Figure 5 is converted into a two-dimensional point cloud. A Monte-Carlo technique is used to place 10 000 squares of a prescribed area randomly within the point cloud domain. The number of particles within each square is measured and a histogram of particle number is created. By varying the area of the squares in the Monte-Carlo simulation one can interrogate the dispersions. In Figure 6b the expected distributions from a truly random dispersion is shown to agree with the Poisson distribution; any dispersion that doesn't can't fairly be termed random. The presence of agglomeration is clear from the spread in the distribution for the largest areas. Another indicator is the most probable number of particles approaching 0 for the smallest areas, which is commensurate with the most probable vacant area. Both are indicators of particle agglomeration and subsequently particle depleted domains. In addition, the two peaks in the distribution that appear for the 4 μm × 4 μm simulation is likely a result of the simulation size coinciding with a characteristic agglomerate spacing. A method to characterize dispersion across length scales is an area of much needed and continued development.

## Effects of Internal Interfaces

Because of the high particle number densities in polymer nanocomposites, the large surface area of the particle/matrix interfaces can dominate the mechanical behavior of the material (a 1–2 vol.-% nanocomposite of 40 nm spherical particles the size of soccer ball[71] has approximately 1 hectare of particle interface area). Often, nanoparticles and polymer matrices are inert by design to limit environmental sensitivity of the tribological response. This inertness affects the nature of the interface and can lead to inherent weakness. Wagner and Vaia articulated the importance of the interface in SWCNT systems. "The presence at the interface of only van der Waals interactions gives interfacial values of less than 3 MPa, whereas the occurrence of covalent bonding for only 1% of the nanotube's carbon atoms to the polymer matrix will give an interfacial strength of 100 MPa".[70] Burris and Sawyer[14] conducted recent studies on alumina-PTFE nanocomposites with particles of varying surface morphology and phase. Particle shape may play an important role on the entanglement of the polymer at the surface and can thus influence the strength of the interface. Figure 7 shows TEM images of these nanoparticles. The first nanoparticle has a reported average particle diameter of 44 nm and a phase reported to be 70:30 Δ:Γ. The second has a reported average particle diameter of 40 nm and is reported to be of 99% α phase. The third has a reported average particle diameter of 80 nm and is reported to be 99% α phase. Histograms are included based on very limited TEM sampling and measurement of particle sizes. The 80 nm alpha particles have been removed from the 40 nm batch, but smaller 40 nm particles appear to remain within the 80 nm batch. The 40 and 80 nm α phase particles appear more faceted and plate-like than the 44 nm Δ:Γ particles, which appear very spherical. These observations are consistent with manufacturer reported morphologies.

Tribological experiments were conducted on nanocomposites of various loadings in standard laboratory conditions at 50 mm · s$^{-1}$ and 6.3 MPa of normal pressure. Wear rate is plotted versus alumina loading in Figure 8. Both the 40 and 80 nm α particles impart dramatic improvements to the wear resistance of PTFE at 0.5% loading. Despite the facts that the nanoparticles all have the same chemical composition and that the sizes of the α particles bound the size of the Δ:Γ particles, the wear rates of the irregular, α phase particle filled nanocomposites are 100–1 000 times lower than for the spherical Δ:Γ phase alumina-filled nanocomposites in all cases. Although characterizations of dispersions are still needed, particle size effects do not appear to be dominant in this case. In a previous publication, we offered the hypothesis that the increased irregularity in shape may lead to improved engagement of the

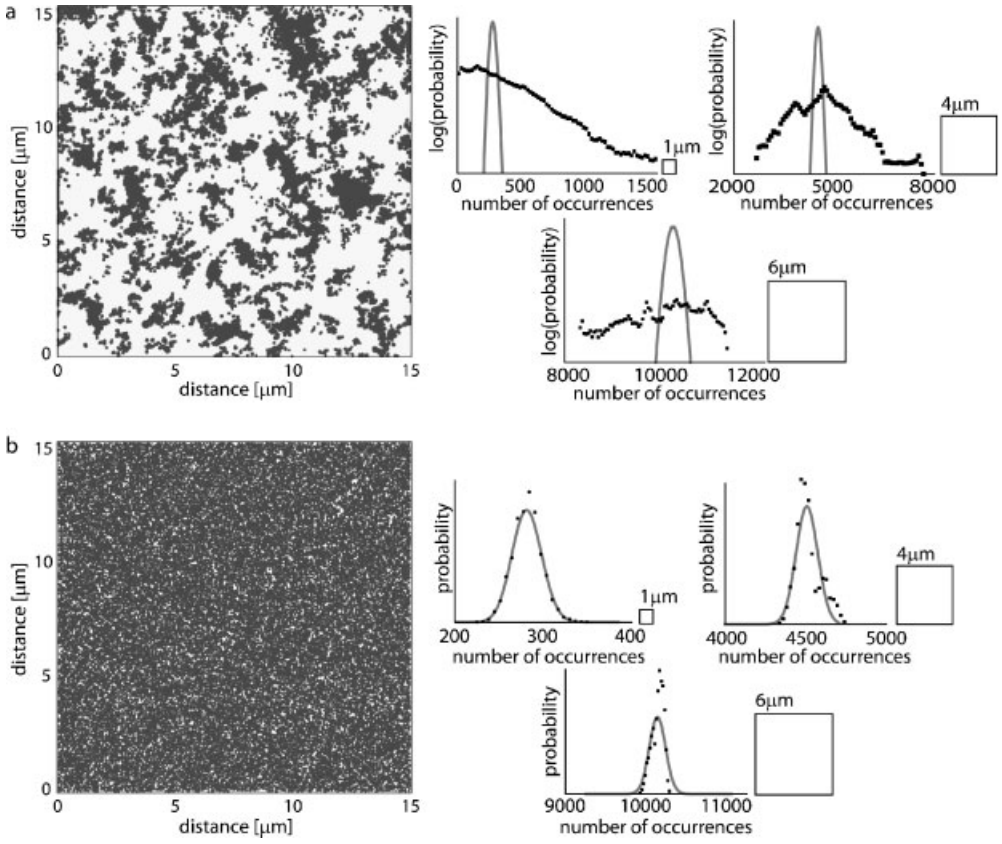


*Figure 6.* Applications of the Monte Carlo analysis method and comparisons to the expected Poisson distribution for the micrograph shown in Figure 4a and a random distribution of the same volume fraction.

PTFE onto the surface of the nanoparticle,[14] but it is unlikely that this mechanism is solely responsible for the 1 000 times improvements in wear resistance. Given that particle phase is varied with particle shape, the chemical reactivity of the nanoparticle surfaces with the PTFE matrix cannot be discarded as a part of the wear reduction mechanism.

## Effects of Phase and Crystallinity

The mechanical effects of nanoparticles are often discussed with regards to wear resistance mechanisms. Some of these effects include lubrication and separation of surfaces,[16] mechanical engagement with the counter-surface,[37] interruption of crack propagation,[53] and

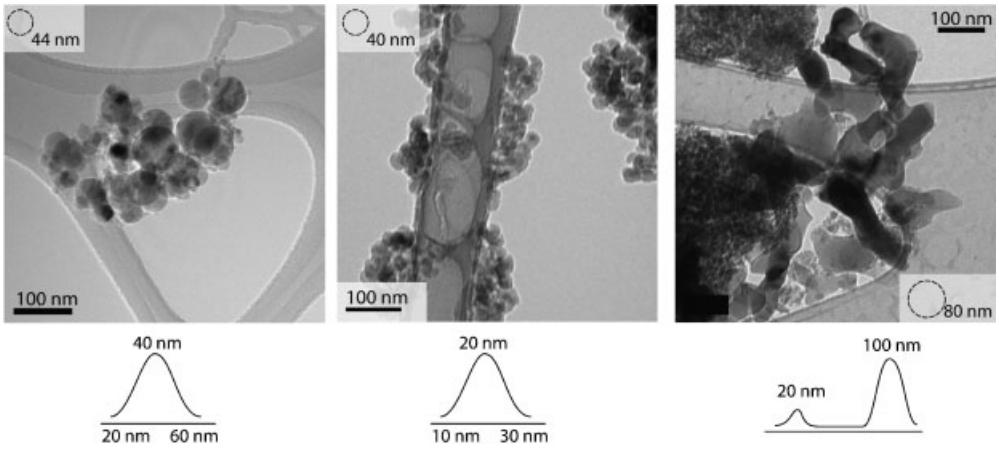


*Figure 7.* Transmission electron images of 44 nm (left), 40 nm (center), and 80 nm (right) particles used in the study.


*Macromol. Mater. Eng.* **2007**, *292*, 387–402

DOI: 10.1002/mame.200600416

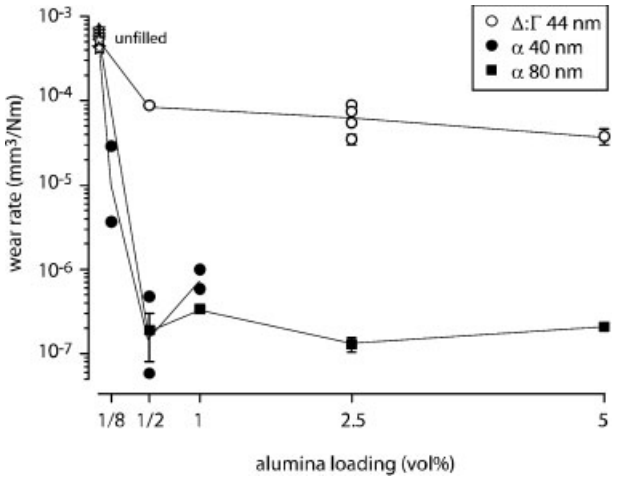


*Figure 8.* Wear rate plotted versus alumina loading for alumina-PTFE nanocomposites with varying nanoparticle morphology. Confidence intervals represent the standard uncertainty in the measurement of wear rate.

prevention of large-scale destruction,[67] to name a few. The potential effects of the nanoparticles on the crystalline phase and morphology of the matrix are rarely discussed in the tribology literature. There are many instances in the macromolecules literature where dramatic changes in the crystallinity and morphology of the matrix as a result of nanoparticle inclusion accompany dramatically altered mechanical properties. Observations include changes in crystallinity, spherulite size, $T_g$, storage modulus, tensile strength, elastic modulus, wear rate, and toughness.[25,34,35,59,60,72]

In tribology, PTFE is a well-known and commonly used polymer for solid lubrication. PTFE is known to have a complex molecular organization, and while it has been shown that crystallinity plays a minimal role on its wear rate,[67] phase and temperature have both been shown to have dramatic influences on the mechanical and tribological properties. Flom and Porile were perhaps the earliest investigators to note a dramatic effect of the phase of PTFE on its tribological properties.[73] They performed sliding experiments with self-mated PTFE at speeds of 11 and 1 890 mm $\cdot$ s$^{-1}$ and found an abrupt and reversible increase in the friction coefficient as the background temperature increased above a threshold value near room temperature in both cases. They hypothesized that the increase was associated with the phase transition from II to IV at 19 °C previously reported by Rigby and Bunn.[74] They further noted a trend of increased friction coefficient with increased sliding velocity. Steijn[75] also found changes in frictional behavior that were associated with phase transitions (II–IV and IV–I) for PTFE. McLaren and Tabor[76] observed increased friction coefficients with increased speed and decreased temperature for self-mated PTFE. Makinson and Tabor[41] combined the early work of Bunn et al.,[77] and Speerschnieder and Li[78] with their own tribological results and electron diffraction work to relate the tribological behavior of PTFE to its crystalline structure. They envisioned a lameller mechanism of motion accommodation where shear in the amorphous regions enables easy sliding of the crystalline domains. More generally, Joyce et al.,[79] Rae and Dattelbaum,[80] Brown and Dattelbaum,[81] Brown et al.,[82] and Rae and Brown[83] found monotonic trends of increased tensile and compressive strength and modulus at decreased temperature. Similar trends have been observed for the friction coefficient and wear rate of PTFE in the range from 200–400 K.[47,53,67,75,84] Brown and Dattelbaum[81] recently published a study investigating the role of crystalline phase on the toughness of PTFE. They found increased fracture toughness for phase I over phase II, especially at high strain rates. Phase II suffers brittle fracture, while the high toughness phase I PTFE is able to fibrillate and bridge cracks, which reduces the effective stress concentrations. These results have important implications to tribology, because the removal of material during wear events is closely related to fracture by requiring energy to create new surfaces. These results also suggest superiority of phase I over II and IV in wear applications, since the events that occur in tribological contacts typically occur with high strain rates. It is hypothesized that a mechanism such as the stabilization of phase I could be responsible for some of the wear reductions in PTFE nanocomposites.

Secondary electron imaging of the wear surface of a 5% 80 nm α phase alumina-PTFE nanocomposite with a wear rate of$\approx 10^{-7}$ mm$^3 \cdot$ N$^{-1} \cdot$ m$^{-1}$[44] was used to investigate the wear mechanisms of these very low-wear PTFE-based materials; Figure 9 shows the results of these observations at two magnifications. In the low magnification image, 'mudflat' cracking is observed on the wear surface. The cracked segments are on the order of tens of micrometers in size and appear as though they could easily be removed, but neither liberated debris nor vacancies on the sample surface are observed. Higher magnification imaging reveals fibrils spanning the cracks, which appears to prevent the liberation of the cracked material as debris. The same alumina-PTFE nanocomposite was fractured by bending at 25 °C and the resulting crack was imaged. This crack is shown in Figure 10. Fibrils are observed to span the entire length of the 150 μm crack. This degree of fibrillation is extraordinary for PTFE under these conditions and suggests that the nanoparticles greatly affect the crystalline morphology and deformation mechanisms of the matrix.

## Quantifying Transfer Films

Transfer film thickness, quality, tenacity and adhesion are often credited with improved tribological performance of

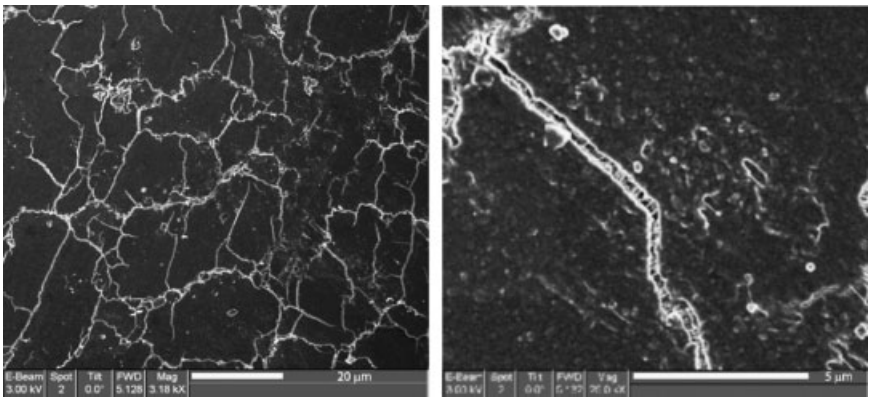


*Figure 9.* SEM images at different magnifications of the worn surface of a 5% 80 nm alpha phase alumina-PTFE nanocomposite. The 'mudflat' cracking is a characteristic that is repeatedly observed for these wear-resistant PTFE nanocomposites. Wear debris appears to be on the order of 1 μm, while the cracking patterns encompass tens of micrometers of material. The liberation of large wear debris appears to be inhibited by fibrils spanning the cracks.

nanocomposite solid lubricants, and are rarely if ever quantified. In 2005, Burris and Sawyer[15] published a study that examined counterface roughness effects on alumina-PTFE nanocomposites. The study showed that these nanocomposites were insensitive to counterface roughness during steady state sliding when thin, and continuous transfer films could be formed. In order to quantify these thin films, scanning white-light interferometry was used to measure transfer film thickness. McElwain[22] recently studied the effect of alumina size on the wear of 2.5% alumina-PTFE composites. Measurements of unfilled, micro-filled and nano-filled PTFE transfer films were made using mapping stylus profilometry. These measurements are shown in Figure 11. Wear rate is plotted versus the maximum transfer film thickness in Figure 12. For both studies it is found that with varying experimental setups and environments, with particles of varying size and phase and varying counterface roughness, wear rate is approximately proportional to the maximum transfer film thickness cubed. These quantitative measurements have provided evidence to support many previous qualitative observations of the relationship between transfer film morphology and wear.

In the macromolecules literature, there are extensive studies that investigate thickness and alignment of model PTFE thin films. It has been well established that under slow ($<$ 10 $mm \cdot s^{-1}$) sliding speeds, the transfer of PTFE can provide an aligned, thin, transfer film for low shear sliding.[85–89] The relationship between transfer film thickness and wear rate suggests that extremely thin and uniform films of PTFE might also be very wear resistant. Recently, experiments were conducted to quantify the tribological properties of model PTFE films to test the hypothesis that thin aligned PTFE films can support low wear sliding.

Model films of PTFE were created by sliding unfilled PTFE against a steel foil at a sliding velocity of 254 $\mu m \cdot s^{-1}$ at 6.35 MPa for 1 000 reciprocation cycles at 25 °C. The resulting film had an average thickness of approximately 50 nm. After creation, the foils were cut into rectangular samples for microtribometry testing. Custom designed sample mounts fixed opposing foils into a crossed-cylinder geometry. This geometry eliminates edge effects, reduces sensitivity to misalignment, and helps reduce average pressures to values more typical of those found in macro-scale testing. Post test analysis of the contact area was used to estimate an average contact pressure of 15 MPa. Two configurations were tested to study the hypothesized frictional anisotropy of aligned PTFE films; parallel and perpendicular. The alignments of the films are in the direction of sliding and against the direction of sliding for the parallel and perpendicular configurations, respectively. Reciprocation experiments on a 600 μm long track with an average sliding speed of 100 $\mu m \cdot s^{-1}$ were conducted for 250 sliding cycles. The results of

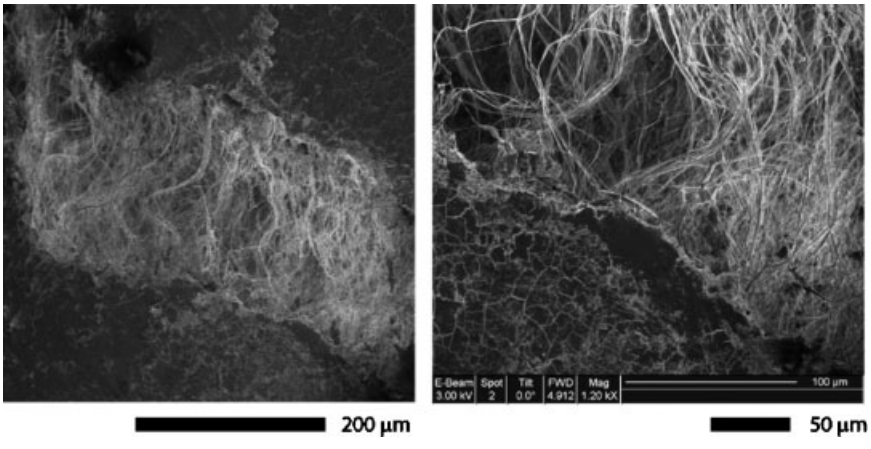


*Figure 10.* SEM images at different magnifications of the worn surface of a 5% 80 nm alpha phase alumina-PTFE nanocomposite after being fractured at room temperature. Fibrils completely span a 150 μm crack. The characteristic 'mudflat' cracking can also be seen on this sample.


*Macromol. Mater. Eng.* **2007**, *292*, 387–402

DOI: 10.1002/mame.200600416

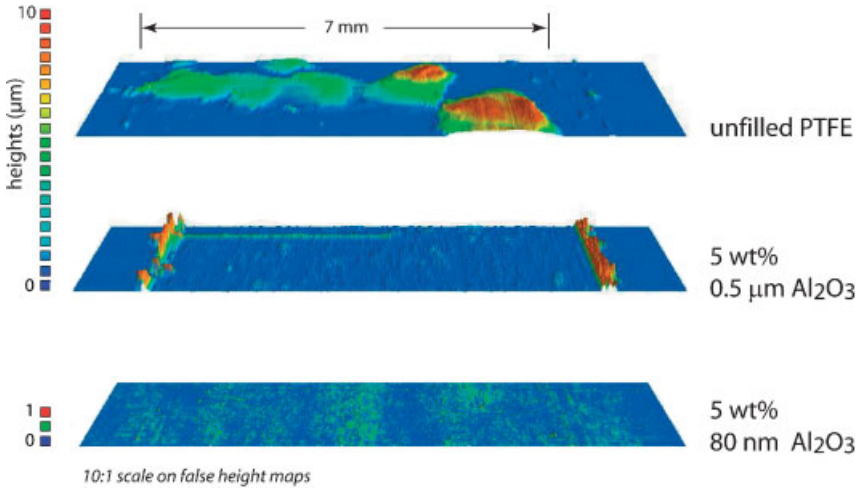


*Figure 11.* Mapping stylus profilometry measurements of transfer films on polished counterfaces from studies by McElwain and Blanchet.[22] Top: Transfer film of unfilled PTFE. Center: 5 wt.-% 500 nm alpha alumina-filled PTFE transfer film. Bottom: 5 wt.-% 80 nm alpha alumina-filled PTFE. The stylus has a 12.5 μm diameter tip and measurements were made using a contacting force of 100 μN.

these experiments are shown in Figure 13.

In line with the hypothesis of frictional anisotropy in PTFE, the perpendicular alignment of the films led to complete failure of the film in about 10 cycles, while parallel aligned films were at least 10 times more wear resistant. Despite having similar average values of friction coefficient for the first few passes, examination of the positionally resolved friction coefficients on the right of Figure 13 reveals that the behaviors are actually quite different. Looking at the first pass, the friction coefficient is nearly constant across the wear track of the parallel aligned sample, while that of the perpendicular aligned sample is more erratic. The mechanism of motion accommodation is clearly more damaging in the case of the perpendicularly aligned films, and the tendency of the film to reorient into the direction of sliding is likely responsible for the erratic friction and wear behavior. The parallel aligned films have much lower wear as a result of stable orientation. However, a simple calculation suggests that the wear rates of parallel aligned films are still orders of magnitude higher for the model PTFE thin films than the wear rates of many of these low wear nanocomposite systems. Since low wear sliding requires the existence of a transfer film, the wear rate of the transfer film itself places a lower limit on the wear rate of the system. From this argument, it can be concluded that thin and aligned transfer films of PTFE are incapable of supporting ultra-low wear sliding. These films must therefore be comprised of some variant of PTFE or composite material.

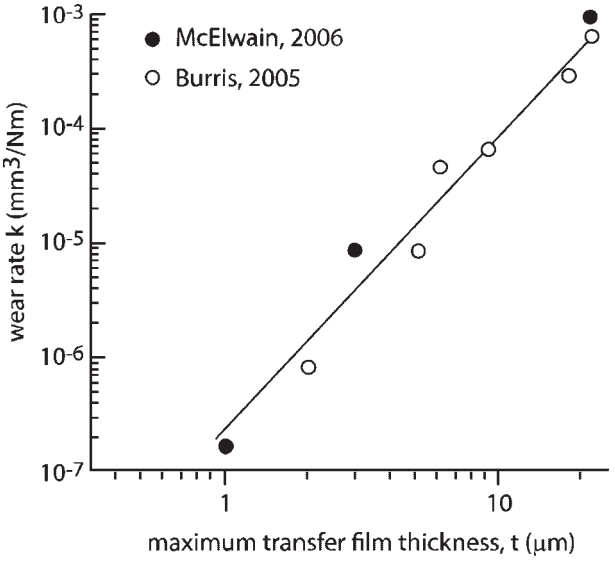


*Figure 12.* Wear rate plotted versus transfer film thickness.[15,22] Wear rates for this system are approximately proportional to the maximum transfer film thickness cubed. No correlation between transfer film thickness and friction coefficient was observed.

To illustrate this point, the same experiments were conducted for a 10 wt.-% PEEK-PTFE[44] composite with a system wear rate of $10^{-7}$ $mm^3 \cdot N^{-1} \cdot m^{-1}$. The results are shown in Figure 14. The composite film has low and stable friction coefficients for the duration of the 1 000 cycle test in both configurations with no obvious signs of wear in post test analysis. Clearly, the compositions and chemistries of these films are additional factors that require quantification for a more complete understanding of these nanocomposite systems. Using X-ray photoelectron spectroscopy, Gong et al.[40,90] and Blanchet and Kennedy[38] found that various micrometer-scale fillers had no influence on the bonding of PTFE at the counterface and concluded that the wear reducing mechanism of the fillers was to disrupt large-scale cohesive failure within the transfer film and bulk rather than to increase adhesion of transfer films to the counterface. It remains an open question as to how composition and chemistry evolve in nanocomposite transfer films and how this evolution influences the sliding wear of polymer nanocomposites.

## Summary

There are currently a number of low-loading, low-wear polymer nanocomposites being synthesized and tested in

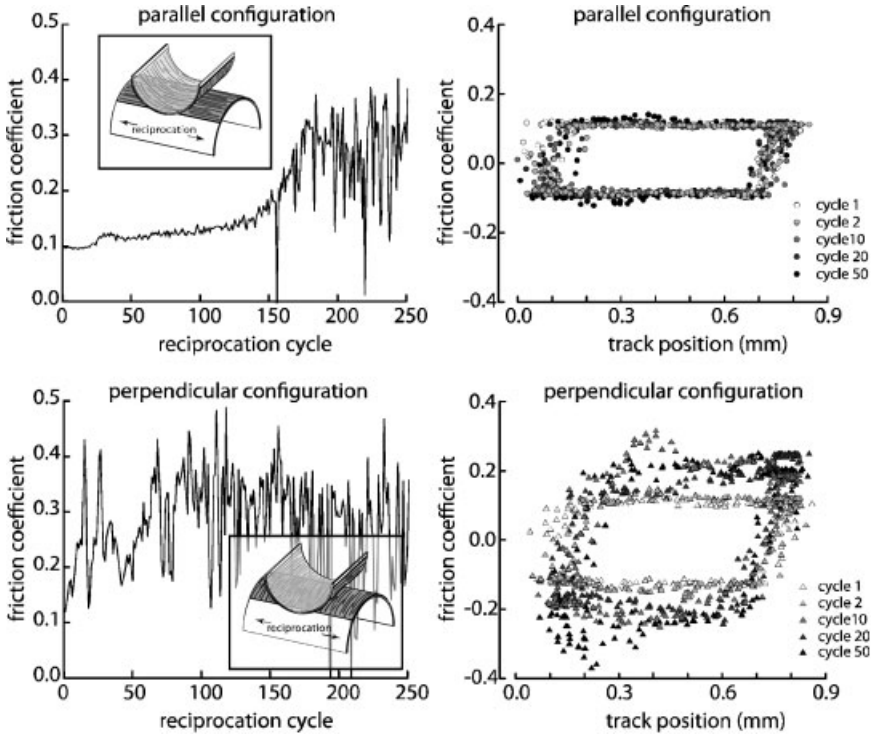


*Figure 13.* Microtribometry friction results for the crossed cylinder oriented PTFE transfer film tests. Friction coefficient is examined versus reciprocation cycle for a) parallel and b) perpendicular configuration. The evolution of friction coefficient along the reciprocation track is also plotted for both the c) parallel and d) perpendicular configurations.

tribology laboratories. Some of these systems outperform traditional microcomposite systems by orders of magnitude with substantially lower filler loadings. Past models using rules of mixtures and mechanical reinforcement are clearly inadequate to describe the phenomena observed in practice. Although there have been recent improvements in our understanding of these systems, nanocomposite design requires more detailed models. There are several aspects of these systems where quantitative measurements can make immediate impact on our understanding of the governing mechanisms. The most obvious need is of standard tools and procedures for quantifying nanoparticle dispersions. These nanoparticle dispersions can dominate the behavior of the composites, yet they are almost completely absent from discussion in the tribology literature. The tools needed for material characterization are currently widely used by the material science community, but need to be implemented more in tribology studies to help clarify experimental results. More thorough characterization of the thermal, morphological, and mechanical behaviors will aid our understanding of the effects of nanoparticles on the matrix. Tools for studying the matrix/filler interface may include atomic force microscopy and transmission electron microscopy and will facilitate a more fundamental understanding of the matrix effects observed in materials characterization. We need more quantitative measurements of the transfer films developed during low wear sliding. These needs include improved thickness and morphology measurements using optical interferometry, stylus profilometry, atomic force microscopy, or nano-indentation. Secondly, quantification of the compositional and chemical evolution of these films is crucial to our understanding of wear resistance in these films. Finally, quantification of fundamental mechanical properties of transfer films is needed to develop models for the tribology of these interfaces at a more detailed level. Combining the tools and techniques of material scientists and tribologists will fulfill many of the needs in nanocomposite tribology and promises to provide profound impacts on our understanding of these complex systems. This new understanding will bring us closer to designing materials for tribological applications.

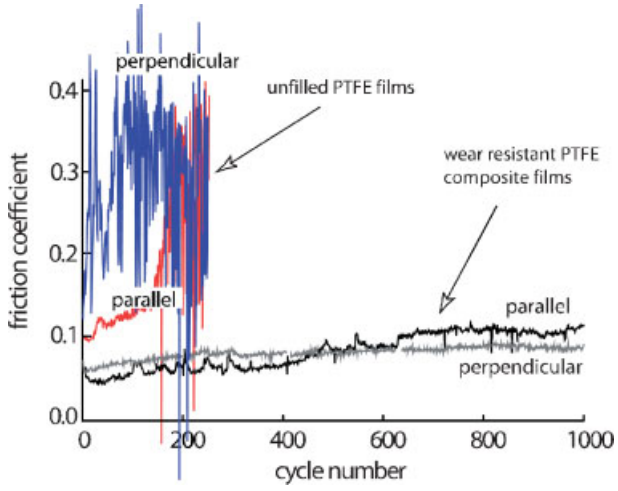


*Figure 14.* Microtribometry measurements of friction coefficients for parallel and perpendicular aligned 10 wt.-%PEEK-PTFE composite transfer films with similar test results of transfer films of unfilled PTFE.

Acknowledgements: This material is based upon an AFOSR-MURI grant FA9550-04-1-0367. Any opinions, findings, and conclusions or recommendations expressed in this material are those of the authors and do not necessarily reflect the views of the Air Force



DOI: 10.1002/mame.200600416

Office of Scientific Research. The authors thank Prof. *Linda Schadler* for helpful collaboration and discussions on interface and morphological effects, and Prof. *Thierry Blanchet* for discussion on PTFE tribology.

Received: November 2, 2006; Revised: January 31, 2007; Accepted: February 7, 2007; DOI: 10.1002/mame.200600416

Keywords: fillers; films; nanocomposites; tribology; wear

[1] P. Feraboli, A. Masini, L. Taraborrelli, A. Pivetti, *Compos. Struct.* **2007**, *78*, 495.
[2] A. Mouritz, E. Gellert, P. Burchill, K. Challis, *Compos. Struct.* **2001**, *53*, 21.
[3] C. C. Baker, J. J. Hu, A. A. Voevodin, *Surf. Coat. Technol.* **2006**, *201*, 4224.
[4] C. Donnet, *Surf. Coat. Technol.* **1996**, *80*, 151.
[5] E. Grossman, I. Gouzman, *Nucl. Instrum. Meth. B* **2003**, *208*, 48.
[6] K. Miyoshi, *Tribol. Int.* **1999**, *32*, 605.
[7] S. Prasad, N. Mcdevitt, J. Zabinski, *Wear* **2000**, *237*, 186.
[8] T. Spalvins, *J. Vacuum Sci. Technol. A* **1987**, *5*, 212.
[9] X. Zhao, Z. Shen, Y. Xing, S. Ma, *Polym. Degrad. Stab.* **2005**, *88*, 275.
[10] D. L. Burris, W. G. Sawyer, *Wear* **2007**, *262*, 220.
[11] A. Cenna, S. Allen, N. Page, P. Dastoor, *Wear* **2001**, *249*, 663.
[12] S. K. Field, M. Jarratt, D. G. Teer, *Tribol. Int.* **2004**, *37*, 949.
[13] J. K. Lancaster, R. W. Bramham, D. Play, R. Waghorne, *J. Lubric. Technol.-T. Asme.* **1982**, *104*, 559.
[14] D. Burris, W. Sawyer, *Wear* **2006**, *260*, 915.
[15] D. Burris, W. Sawyer, *Tribol. Trans.* **2005**, *48*, 147.
[16] W. Chen, F. Li, G. Han, J. Xia, L. Wang, J. Tu, Z. Xu, *Tribol. Lett.* **2003**, *15*, 275.
[17] D. F. Eckel, M. P. Balogh, D. Fasulo, W. R. Rodgers, *J. Appl. Polym. Sci.* **2004**, *93*, 1110.
[18] A. Eitan, F. Fisher, R. Andrews, L. Brinson, L. Schadler, *Compos. Sci. Technol.* **2006**, *66*, 1162.
[19] T. D. Fornes, J. Yoon, H. Keskkula, D. R. Paul, *Polymer* **2001**, *42*, 9929.
[20] F. Li, K. Hu, J. Li, B. Zhao, *Wear* **2001**, *249*, 877.
[21] N. L. Mccook, B. Boesl, D. L. Burris, W. G. Sawyer, *Tribol. Lett.* **2006**, *22*, 253.
[22] S. Mcelwain, *M.Sc. Thesis*, Rensselaer Polytechnic Institute, Troy, New York 2006.
[23] C. Ng, L. Schadler, R. Siegel, *Nanostruct. Mater.* **1999**, *12*, 507.
[24] E. Petrovicova, R. Knight, L. Schadler, T. Twardowski, *J. Appl. Polym. Sci.* **2000**, *78*, 2272.
[25] D. Ratna, S. Divekar, A. Samui, B. Chakraborty, A. Banthia, *Polymer* **2006**, *47*, 4068.
[26] E. Reynaud, T. Jouen, C. Gauthier, G. Vigier, J. Varlet, *Polymer* **2001**, *42*, 8759.
[27] W. Sawyer, K. Freudenberg, P. Bhimaraj, L. Schadler, *Wear* **2003**, *254*, 573.
[28] R. Siegel, S. Chang, B. Ash, J. Stone, P. Ajayan, R. Doremus, L. Schadler, *Scripta Mater.* **2001**, *44*, 2061.
[29] O. Wang, Q. Xue, W. Shen, *Tribol. Int.* **1997**, *30*, 193.
[30] Q. Wang, J. Xu, W. Shen, W. Liu, *Wear* **1996**, *196*, 82.
[31] Q. Wang, Q. Xue, H. Liu, W. Shen, J. Xu, *Wear* **1996**, *198*, 216.
[32] Q. Wang, Q. Xue, W. Liu, J. Chen, *Wear* **2000**, *243*, 140.
[33] Q. Xue, Q. Wang, *Wear* **1997**, *213*, 54.
[34] K. Yang, Q. Yang, G. Li, Y. Sun, D. Feng, *Mater. Lett.* **2006**, *60*, 805.
[35] A. Yasmin, J. Luo, J. Abot, I. Daniel, *Compos. Sci. Technol.* **2006**, *66*, 2415.
[36] S. Bahadur, *Wear* **2000**, *245*, 92.
[37] S. Bahadur, D. Tabor, *Wear* **1984**, *98*, 1.
[38] T. Blanchet, F. Kennedy, D. Jayne, *Tribol. Trans.* **1993**, *36*, 535.
[39] B. Briscoe, *Tribol. Int.* **1981**, *14*, 231.
[40] D. Gong, Q. Xue, H. Wang, *Wear* **1991**, *148*, 161.
[41] K. Makinson, D. Tabor, *Nature* **1964**, *201*, 464.
[42] Y. Wang, F. Yan, *Wear* **2006**, *261*, 1359.
[43] T. Schmitz, J. Action, J. Ziegert, W. Sawyer, *J. Tribol., Trans. ASME* **2005**, *127*, 673.
[44] D. Burris, W. Sawyer, *Wear* **2006**, *261*, 410.
[45] T. Schmitz, J. Action, D. Burris, J. Ziegert, W. Sawyer, *J. Tribol., Trans. ASME* **2004**, *126*, 802.
[46] Z. Lu, K. Friedrich, *Wear* **1995**, *181*, 624.
[47] N. Mccook, D. Burris, G. Bourne, J. Steffens, J. Hanrahan, W. Sawyer, *Tribol. Lett.* **2005**, *18*, 119.
[48] B. Menzel, T. Blanchet, *Lubrication Eng.* **2002**, *58*, 29.
[49] M. Palabiyik, S. Bahadur, *Wear* **2000**, *246*, 149.
[50] J. Bijwe, S. Sen, A. Ghosh, *Wear* **2005**, *258*, 1536.
[51] B. Briscoe, L. Yao, T. Stolarski, *Wear* **1986**, *108*, 357.
[52] K. Friedrich, Z. Lu, A. Hager, *Wear* **1995**, *190*, 139.
[53] T. Blanchet, F. Kennedy, *Wear* **1992**, *153*, 229.
[54] J. Khedkar, I. Negulescu, E. Meletis, *Wear* **2002**, *252*, 361.
[55] F. Li, F. Yan, L. Yu, W. Liu, *Wear* **2000**, *237*, 33.
[56] N. Sung, N. Suh, *Wear* **1979**, *53*, 129.
[57] S. Zhang, *Tribol. Int.* **1998**, *31*, 49.
[58] T. Agag, T. Koga, T. Takeichi, *Polymer* **2001**, *42*, 3399.
[59] B. Ash, L. Schadler, R. Siegel, *Mater. Lett.* **2002**, *55*, 83.
[60] P. Bhimaraj, D. Burris, J. Action, W. Sawyer, C. Toney, R. Siegel, L. Schadler, *Wear* **2005**, *258*, 1437.
[61] C. Schwartz, S. Bahadur, *Wear* **2000**, *237*, 261.
[62] K. Tanaka, S. Kawakami, *Wear* **1982**, *79*, 221.
[63] S. Bahadur, V. Polineni, *Wear* **1996**, *200*, 95.
[64] T. Blanchet, Y. Peng, *Wear* **1998**, *214*, 186.
[65] X. Liu, T. Li, N. Tian, W. Liu, *J. Appl. Polym. Sci.* **1999**, *74*, 747.
[66] X. X. Liu, T. S. Li, X. J. Liu, R. G. Lv, *Macromol. Mater. Eng.* **2005**, *290*, 172.
[67] K. Tanaka, Y. Uchiyama, S. Toyooka, *Wear* **1973**, *23*, 153.
[68] H. R. Dennis, D. L. Hunter, D. Chang, S. Kim, J. L. White, J. W. Cho, D. R. Paul, *Polymer* **2001**, *42*, 9513.
[69] A. Karnezis, G. Durrant, B. Cantor, *Mater. Charact.* **1998**, *40*, 97.
[70] D. Wagner, R. Vaia, *Mater. Today* **2004**, 38.
[71] P. Neilson, R. Jones, P. I. Mech, *Eng. B-J. Eng.* **2003**, *217*, 715.
[72] H. Koerner, W. Liu, M. Alexander, P. Mirau, H. Dowty, R. Vaia, *Polymer* **2005**, *46*, 4405.
[73] D. Flom, N. Porile, *J. Appl. Phys.* **1955**, *26*, 1088.
[74] H. Rigby, C. Bunn, *Nature* **1949**, *164*, 583.
[75] R. Steijn, *ASLE Trans.* **1968**, *11*, 235.
[76] K. Mclaren, D. Tabor, *Nature* **1963**, *197*, 856.
[77] C. Bunn, A. Cobbold, R. Palmer, *J. Polym. Sci.* **1958**, *28*, 365.

[78] C. Speerschneider, C. Li, *J. Appl. Phys.* **1962**, *33*, 1871.
[79] J. Joyce, *Polym. Eng. Sci.* **2003**, *43*, 1702.
[80] P. Rae, D. Dattelbaum, *Polymer* **2004**, *45*, 7615.
[81] E. Brown, D. Dattelbaum, *Polymer* **2005**, *46*, 3056.
[82] E. Brown, P. Rae, E. Orler, G. Gray, D. Dattelbaum, *Mater. Sci. Eng., C* **2006**, *26*, 1338.
[83] P. Rae, E. Brown, *Polymer* **2005**, *46*, 8128.
[84] V. Smurugov, A. Senatrev, V. Savkin, V. Biran, A. Sviridyonok, *Wear* **1992**, *158*, 61.
[85] G. Beamson, D. Clark, D. Deegan, N. Hayes, D. Law, J. Rasmusson, W. Salaneck, *Surf. Interface Anal.* **1996**, *24*, 204.
[86] D. Breiby, T. Solling, O. Bunk, R. Nyberg, K. Norrman, M. Nielsen, *Macromolecules* **2005**, *38*, 2383.
[87] C. Pooley, D. Tabor, *Proc. R. Soc. London, Ser. A* **1972**, *329*, 251.
[88] D. Wheeler, *Wear* **1981**, *66*, 355.
[89] J. Wittmann, P. Smith, *Nature* **1991**, *352*, 414.
[90] D. L. Gong, B. Zhang, Q. J. Xue, H. L. Wang, *Wear* **1990**, *137*, 25.



DOI: 10.1002/mame.200600416